HOSTED BY
ELSEVIER
CrossMark
Available online at www.sciencedirect.com
ScienceDirect
Defence Technology 11 (2015) 299–307
www.elsevier.com/locate/dt

Pitting corrosion resistance and bond strength of stainless steel overlay by friction surfacing on high strength low alloy steel

Amit Kumar SINGH [a,*], G. Madhusudhan REDDY [a], K. Srinivas RAO [b]

[a] *Defence Metallurgical Research Laboratory, Hyderabad, A.P. 500058, India*
[b] *Andhra University, Visakapatnam, A.P. 530003, India*

Received 13 May 2015; revised 30 May 2015; accepted 3 June 2015
Available online 2 July 2015

Abstract

Surface modification is essential for improving the service properties of components. Cladding is one of the most widely employed methods of surface modification. Friction surfacing is a candidate process for depositing the corrosion resistant coatings. Being a solid state process, it offers several advantages over conventional fusion based surfacing process. The aim of this work is to identify the relationship between the input variables and the process response and develop the predictive models that can be used in the design of new friction surfacing applications. In the current work, austenitic stainless steel AISI 304 was friction surfaced on high strength low alloy steel substrate. Friction surfacing parameters, such as mechtrode rotational speed, feed rate of substrate and axial force on mechtrode, play a major role in determining the pitting corrosion resistance and bond strength of friction surfaced coatings. Friction surfaced coating and base metal were tested for pitting corrosion by potentiodynamic polarization technique. Coating microstructure was characterized using optical microscopy, scanning electron microscopy and X-ray diffraction. Coatings in the as deposited condition exhibited strain-induced martensite in austenitic matrix. Pitting resistance of surfaced coatings was found to be much lower than that of mechtrode material and superior to that of substrate. A central composite design with three factors (mechtrode rotational speed, substrate traverse speed, axial load on mechtrode) and five levels was chosen to minimize the number of experimental conditions. Response surface methodology was used to develop the model. In the present work, an attempt has been made to develop a mathematical model to predict the pitting corrosion resistance and bond strength by incorporating the friction surfacing process parameters.

Keywords: Friction surfacing; Coating; Pitting corrosion resistance; Response surface methodolgy

1. Introduction

The surfaces of engineering materials are given the specific treatments that are different from those of the core. These treatments can alter the composition of the case by incorporating the specific species on the surface of the substrate material or it can be subjected to heat treatment which do not alter the composition of the substrates or the deposited layer can have a different material than the substrate. The surface treatments can be physical, physico–chemical, fusion, as well as non-fusion based. Solid state process that does not involve melting and solidification is versatile as it gives rise to the deposits which are free from solidification related defects it is an amenable process for many incompatible dissimilar metals owing to the short interaction time available for the extensive formation of deleterious intermetallics. Friction surfacing is one such solid state process currently being pursued extensively for various surfacing applications requiring wear and corrosion resistance properties. A schematic diagram of the surfacing process is shown in Fig. 1. The friction surfacing process involves a rotating coating rod called mechtrode that is brought in contact with the substrate under axial load. Intense friction heat is produced on the rubbing surface between the

* Corresponding author. Tel.: +91 4024586604; fax: +91 4024342697.
E-mail addresses: amitsinghdrdo@gmail.com (A.K. SINGH), gmreddy_dmrl@yahoo.co.in (G.M. REDDY), arunaraok@yahoo.com (K.S. RAO).
Peer review under responsibility of China Ordnance Society.

http://dx.doi.org/10.1016/j.dt.2015.06.002

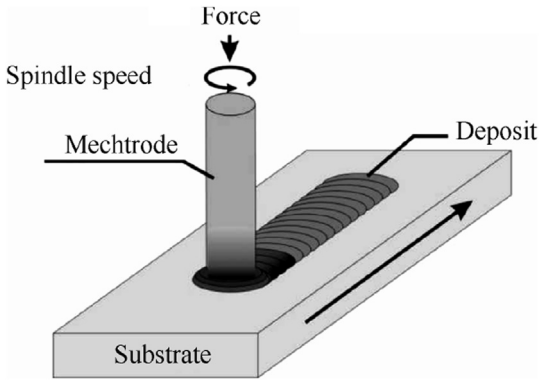

Fig. 1. Friction surfacing process.

substrate and the coating rod. Generated heat is sufficient to plastically deform the end of the mechtrode. A layer of mechtrode material is deposited by moving the substrate across the face of the rotating rod. Metal coatings are made possible by the generation of high contact stress and intimate contact between the coating material and substrate which initiates solid-state adhesion between the coating and the substrate [1]. Being a solid state process, the friction surfacing offers several advantages over conventional fusion welding processes. Friction surfaced coatings exhibit zero dilution and wrought microstructures with very fine grain size. Since melting and solidification are not involved, the problems, such as solidification cracking, brittle intermetallic formation and porosity, do not arise. The critical areas of application include the deposition of hard facing materials on cutting edges of knives of various categories, punch, die, tools and blades required for food processing, chemical, agriculture and medical industries. It opens up a new area of repair and reclamation of worn and damaged components [2,3].

However, the use of friction surfacing process for many applications has been limited due to the difficulty of monitoring and control of the process outputs, such as bond quality and coating dimensions [4]. Proper selection of process parameters is vital for obtaining the quality coatings using friction surfacing. Selection of process parameters and torque-time characteristic are important for the quantum of heat generated at the contact surface and to maintain consumable at quasi steady status in entire process, which affect the quality of deposit [5].The three main friction surfacing parameters are rotational speed of mechtrode, substrate traverse speed and axial force on mechtrode by means of which the desired quality of the coating layer with improved bond strength and corrosion resistance can be achieved [6,7]. Empirical investigations are normally required to determine the optimum parameters that produce the required process response.

High strength low alloy steel is widely used due to easy availability and good weldability. Corrosion resistance of low alloy steel can be improved by surface coating with stainless steel, high speed steel, tool steel and metal matrix composites [6–8]. A number of successful research studies on friction surfacing of similar and dissimilar combinations have been done especially in the areas of microstructural analysis of coating and mechanism during process [9,10]. However very few systematic studies have been performed on relationship between the various process parameters and resulting properties, especially bond strength and corrosion resistance. In the present study, AISI 304 was chosen considering its widespread industrial use as corrosion resistant clad material for high strength low alloy steels. This investigation is aimed at studying the microstructure, pitting corrosion resistance and bond integrity of friction surfaced austenitic stainless steel 304 coatings produced on high strength low alloy steel substrate in detail.

Table 1
Chemical composition of materials.

Materials	Elements/wt. %							
	C	Si	Mn	Ni	Cr	P	S	Fe
High strength low alloy steel(substrate)	0.08	0.3	1.5	0.8	0.3	0.015	0.012	Rest
AISI304(mechtrode)	0.05	1.0	1.0	8.0	18	0.045	0.03	Rest

2. Materials and experiment

The stainless steel AISI 304 (15 mm diameter and 250 mm length) and the low alloy steel plate (10 mm × 100 mm × 250 mm) are used as mechtrode and substrate, respectively. The chemical compositions of materials are shown in Table 1. The experiments are carried out using friction surfacing machine (50 kN capacity), specially designed and developed by Defence Metallurgical Research Laboratory, Hyderabad, India.

Trial experiments are conducted to determine the working range of the factors, such as rotational speed of mechtrode (A), substrate traverse speed (B) and axial force on mechtrode (C). Feasible limits of the parameters are chosen in such a way that the coating should be free from any visible defects.

In the present study, the temperature measurements were carried out close to the rubbing end of the rotating mechtrode using a caliberated infrared camera capable of measuring the temperatures up to 1500 °C. The setup is shown in Fig. 2. The camera was focused at the rotating mechtrode/substrate interface.

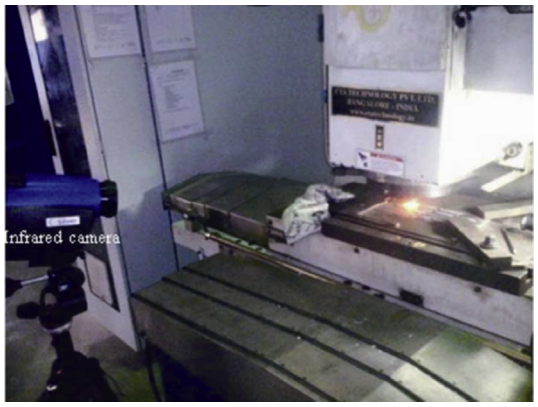

Fig. 2. Experimental setup for temperature measurements during friction surfacing.

Table 2
Factors and levels of the experimental design.

S. No.	Factors	Levels				
		(−2)	(−1)	(0)	(+1)	(+2)
1	Mechtrode rotational speed *A*/rpm	1100	1200	1300	1400	1500
2	Substrate traverse speed *B*/(mm· min^{-1})	100	125	150	175	200
3	Axial force *C*/kN	30	35	40	45	50

Statistical design of experiment approach is used to minimize the number of trials required to optimize surfacing conditions. The three important parameters, i.e., rotational speed of mechtrode, traverse speed of substrate and axial load, were selected for the experimentation. Central composite design was chosen with three process parameters varying at five levels [11]. The generalized regression equation of experiment [12] is given as

$$Y = b_0 + \sum b_i x_i + \sum b_{ij} x_i^2 + \sum b_{ij} x_i x_j$$

where Y is the response function, and $b_i (i = 0, 1, 2, 3)$ is the unknown coefficient that is estimated by least square fitting of the model to the experimental results obtained at the design points. Table 2 indicates the selected factors and corresponding levels against which experimental design is prepared. Table 3 shows the 20 set of coded conditions used to form the design matrix and output value as pitting potential and bond strength. The friction surfaced coatings were subjected to ultrasonic testing (UT) by employing a specially developed calibration block in accordance with ASTM A578M. The good bond area was subjected to further investigation. Transverse section of friction surfaced coating was prepared using standard metallographic technique for microstructural examination. X-ray diffraction studies on friction surfaced coating were carried to identify various phases present by using Cu Kα radiation on a Philips X'Pert Pro diffractometer. To evaluate the integrity of the friction surfaced coatings, the ram tensile test (Fig. 3) was carried out to find the tensile strength of the coating by employing specially designed ram tensile fixture. The ram tensile test specimens were prepared as per MIL-J-24445 (SH) standard.

Table 3
Design matrix and measured bond strength and pitting corrosion resistance.

Run	Mechtrode rotational speed *A*/rpm	Substrate traverse speed *B*/(mm· min^{-1})	Axial force *C*/kN	Bond strength /MPa	Pitting corrosion resistance/mV
1	1200	125	35	248	544.16
2	1400	125	35	350	478.48
3	1200	175	35	365	368.48
4	1400	175	35	389	370.4
5	1200	125	45	375	441.76
6	1400	125	45	364	429.9
7	1200	175	45	419	384.9
8	1400	175	45	349	366.94
9	1300	150	40	238	430.16
10	1100	150	40	321	441.47
11	1500	150	40	342	404.36
12	1300	100	40	451	415.83
13	1300	200	40	500	415.83
14	1300	150	30	487	488.99
15	1300	150	50	413	475.88
16	1300	150	40	416	432.50
17	1300	150	40	417	430.50
18	1300	150	40	414	431.00
19	1300	150	40	413	433.00
20	1300	150	40	415	427.50

Pitting resistance for base metal (low alloy steel) No passivation
Pitting resistance for mechtrode (AISI 304) 715.00 mV

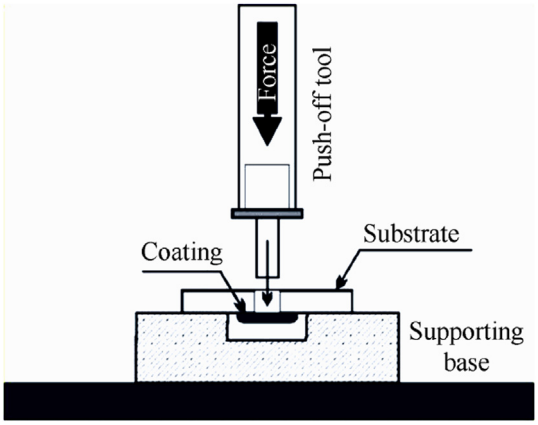

Fig. 3. Schematic diagram of ram tensile test.

A software-based GillAc basic electrochemical system was used to conduct potentiodynamic polarization tests to study the pitting corrosion behaviors of polished samples of friction surfaced coatings. All experiments were conducted in an electrolyte of 0.5M H_2SO_4 + 0.5M NaCl. Steady state potential was recorded 10 min after immersion of specimen into the electrolyte, and the potential was raised anodically at a scan rate of 2m· Vs^{-1}. The potential at which the current increases abruptly after the passive region was taken as pitting potential E_{pit}. Specimens that exhibited higher positive potential were considered to have better pitting corrosion resistance.

3. Results and discussion

3.1. Microstructure

A typical friction surfaced coating is shown in Fig. 4. As can be seen, the coating is bonded well with the substrate without any physical discontinuities except at the edges (for about 0.2 mm on either side). Fig. 5(a) shows the coating/substrate interface macrostructure. Interface (Fig. 5(b)) is

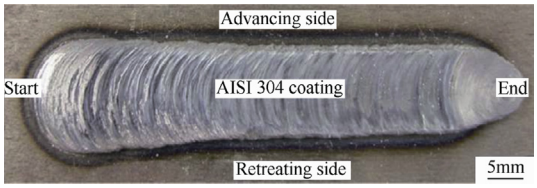

Fig. 4. Typical friction surfaced coating of AISI 304 stainless steel (top view).

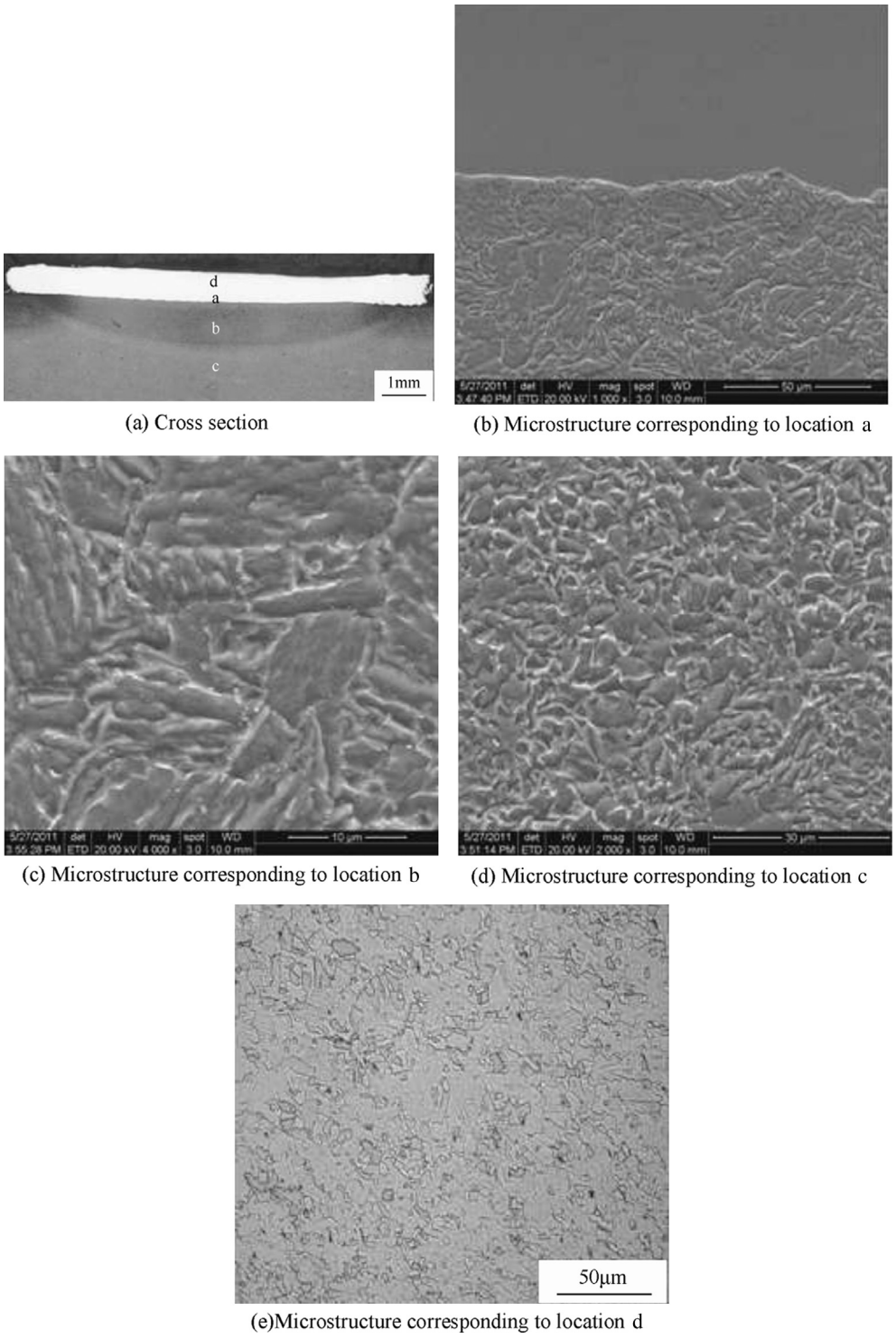

(a) Cross section

(b) Microstructure corresponding to location a

(c) Microstructure corresponding to location b

(d) Microstructure corresponding to location c

(e)Microstructure corresponding to location d

Fig. 5. Friction surfaced stainless steel coating. Note: the substrate is etched with 2% nital while the coating is in as-polished condition.

observed to be relatively uniform with good coating integrity. No oxide inclusions are observed at interface region. Fig. 5(c) and (d) show the microstructures of HAZ and base metal. Grain coarsening is observed in the substrate close to the coating interface. Fine grained austenitic structure was observed and is due to dynamic recrystallization that occurs during friction surfacing (Fig. 5(e)).

XRD studies were carried out to assess the presence of δ ferrite in the deposited austenitic matrix. XRD studies of friction surfaced coating confirmed the absence of δ ferrite and the presence of strain-induced martensite (Fig. 6). The absence of δ ferrite in friction surfaced coatings clearly established that the temperature (1000 °C) generated during friction surfacing has not exceeded the limit (1200 °C)

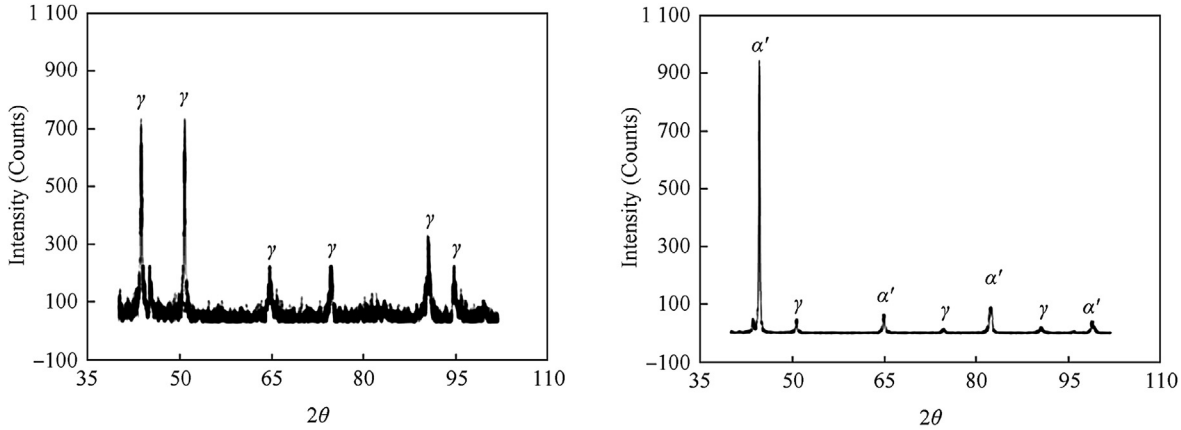

Fig. 6. X-ray diffraction.

required for the formation of δ ferrite, and suggest that the mechtrode was not heated well into the δ ferrite + γ field during friction surfacing. This was confirmed by measuring the temperature at the rubbing end of the rotating mechtrode using infrared thermography (Fig. 7). The absence of δ ferrite in friction surfaced coating is beneficial in improving the corrosion resistance compared to fusion based cladding process.

3.2. Pitting corrosion resistance

Typical polarization curves for base materials and surface coatings are presented in Figs. 8 and 9. Pitting potential E_{pit} was taken as the criterion for comparison of pitting corrosion resistance (Table 3). Less positive potential E_{pit} values imply lower resistance to pitting, and vice versa. When stainless steel is in contact with aqueous environment, the passive film of chromium oxide offers better corrosion resistance. However the passive film may break locally at selected locations due to the weakling of passive film at heterogeneities in the material like precipitates, grain boundaries, inclusions, segregation, etc. The other reason for localized corrosion of stainless steel is accumulation of chloride ions at the surface heterogeneities and favorable locations.

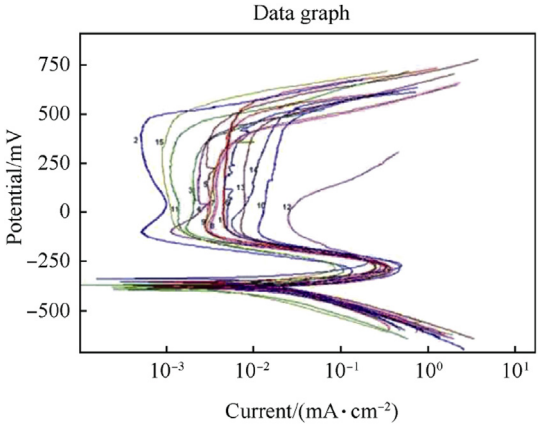

Fig. 8. Polarization behavior of friction surfaced coatings produced by various process parameters (1–15) as per design matrix.

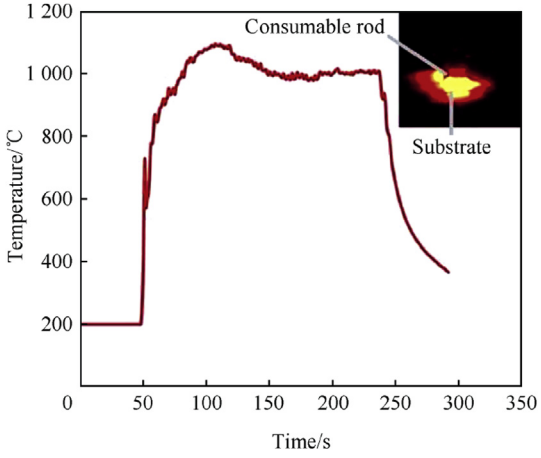

Fig. 7. Thermal profile obtained from the interface of mechtrode rod/substrate temperature close to the rubbing end of the rotating mechtrode as a function of time.

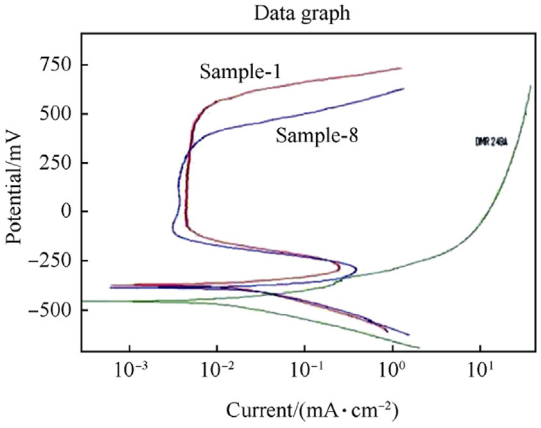

Fig. 9. Polarization behavior of substrate material (DMR 249A—high strength low alloy steel), friction surfaced coatings [high pitting corrosion resistance -sample 1(1200 rpm, 125 mm/s, 35 kN)]; [low pitting corrosion resistance -sample 8(1400 rpm, 175 mm/s, 45 kN)].

Table 3 shows the pitting potentials of base metal, mechtrode material and friction surfaced coatings. Pitting resistance of surfaced coatings was found to be much lower than that of mechtrode material. In general it is a well-known fact that the microstructural changes that occur during friction surfacing process strongly affect the corrosion behavior of any alloy. In the present study, the microstructural change is attributed to high strain rate and dynamic recrystallization that occurs during friction surfacing. It is likely that the influences of high strain rates and dynamic recrystallization can cause the microstructural change in coatings. Relatively high magnitude of plastic strains are generally induced in friction surfaced coatings because of sever plastic deformation. These plastic strains may in turn also contribute to the formation of strain-induced martensite in the friction surfaced coating. XRD results (Fig. 6) clearly reveals the evidence of martensite formation in the austenitic matrix of surfaced coating.

Pitting potential data (Table 3) clearly indicates that the pitting corrosion resistance decreases with the increase in rotational speed of mechtrode. Among the friction surfacing process parameters, a variable that influences strain rate is only the rotational speed. It is a fact that the strain rate of plastic deformation during friction surfacing increases and leads to enhancement in the strain energy and an amount of strain-induced martensite in the austenitic matrix as the rotational speed of mechtrode increases. One of the possible sources of pit initiation is at the interface between strain-induced martesite and austentic matrix. Strain-induced martensite acts as active anodic site in the electrochemical reaction and thus results in severe localized corrosion. A similar phenomenon is noticed in stainless steels by increasing cold working above 23% [13].

The pit density evidence (Fig. 10) clearly confirmed that the combination of lower mechtrode rotational speed and relatively higher substrate traverse speed improves the pitting corrosion resistance. Higher lattice mismatch at the interface of martensite/austenite matrix results in localized disturbance of passive film, which leads to severe pitting corrosion. This lattice mismatch is also due to relatively high strain energy difference between martensite and austenite grain boundary. Since the interface have higher value of strain energy compared to the inner portion of the austenite away from the grain boundary regions, and hence this strain energy is generally a driving force for electrochemical reaction leading to localized pitting corrosion resistance of stainless steels [14]. Combination of higher mechtrode rotational speed and lower substrate traverse speed during friction surfacing resulted in a poor pitting resistance of surfaced coatings.

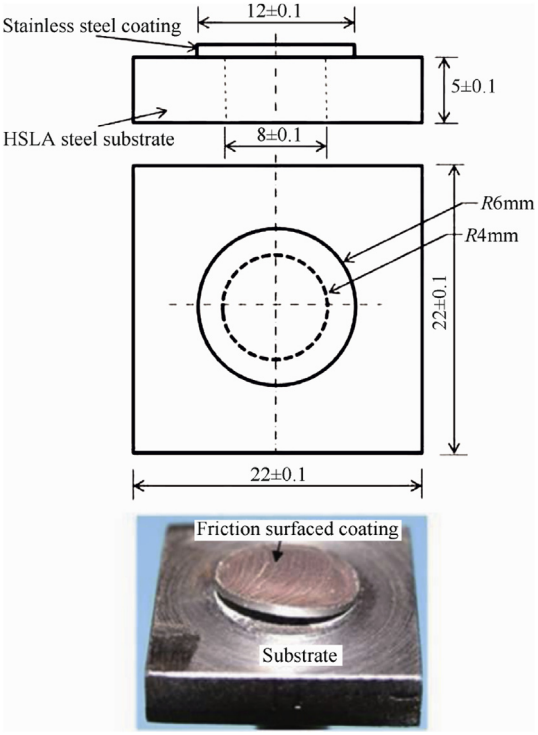

Fig. 11. Typical drawing and picture of ram tensile sample.

The other possible mechanism is related to the accumulation of chloride ions at favorable locations on the surfaced coating. In the present work, a pitting corrosion test was carried out using potentiodynamic polarization method in the chloride environment (0.5 M NaCl). Harmful anions, the most notable Cl^- ion, have been shown to cause the chemical breakdown of passive oxide film on stainless steels [15,16]. In friction surfaced coatings, internal stresses, often approaching the yield strength, may be produced [17]. Anions will migrate to stress gradient locations, which results in the localized

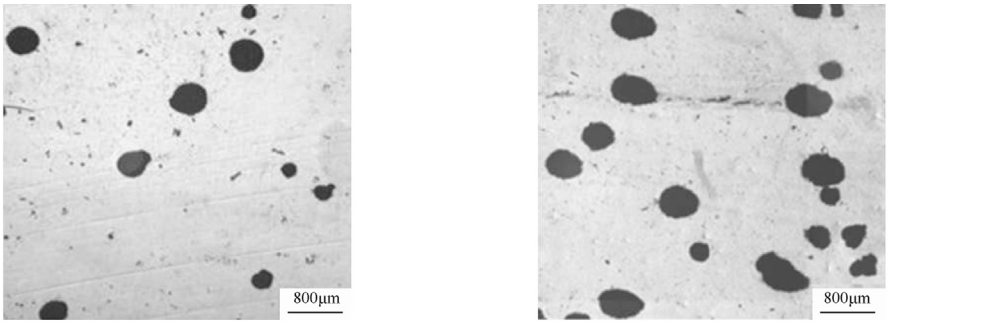

(a) High corrosion resistance sample (1200 rpm, 125mm/s,35 kN) (b) Low corrosion resistance sample (1400 rpm, 175mm/s,45 kN)

Fig. 10. Optical micrographs of corroded surfaces of friction surfaced coatings.

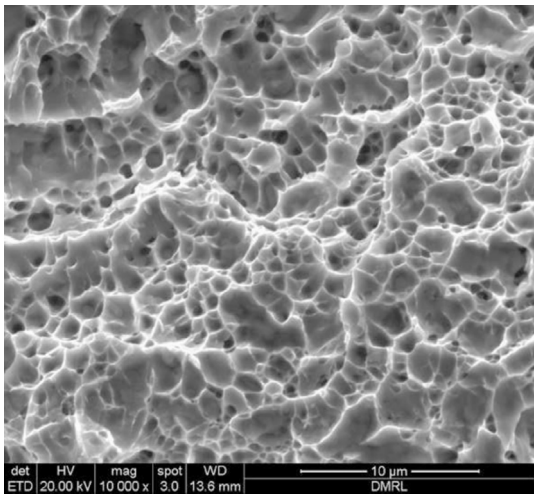

Fig. 12. Fractograph of tested bond sample with high bond strength (1300 rpm, 200 mm/s, 40 kN).

regions of high anion concentration and the saline electrolytes; the electrolysis reactions from corrosion can produce the localized regions. Passivation breakdown in association with lack of spontaneous re-passivation in the presence of such electrolytes promotes an accelerated localized attack [18]. This is in agreement with the present results on pitting corrosion of friction surfaced stainless steel coatings. In view of the above, it is clearly understood that the friction surfaced stainless steel coatings exhibit poor pitting resistance compared to uncoated stainless steel.

3.3. Bond strength

Among various mechanical test methods, like shear strength test, bend test, chisel test, etc., available for assessing the bond strength of claded joint, a tensile test method called ' Ram tensile test' developed by Enright et al. [19] is considered to be the more meaningful test. Ram tensile test method ensures failure of the specimen in the bond zone by a pure tensile load which represents the strength of the bond. The bond strength of coated specimen is shown in Table 3. From Table 3 it can be inferred that the maximum shear strength of 500 MPa and the minimum shear strength of 238 MPa were obtained on the friction surfaced alloy AISI 304 coatings produced in the current study. All ram tensile test specimens were observed to fail at the coating/substrate interface. Typical drawing and picture of ram tensile test specimen are shown in Fig. 11. The fractographs for high bond strength specimen, presented in Fig. 12, shows the features of fracture containing ductile micro-voids.

3.4. Interpretation of response surface models

The effects of various friction surfacing parameters, viz. mechtrode rotational speed, substrate traverse speed and axial force, were evaluated with respect to pitting corrosion resistance and bond strength from the response surface models (Figs. 13 and 14). These models can help in predicting the pitting corrosion resistance and bond strength at any zone of the experimental domain. The variation of temperature at the bond interface with thermo-physical properties (mechtrode

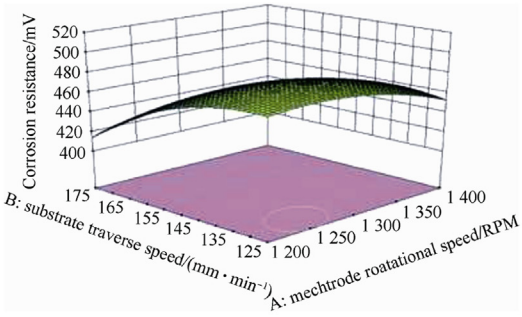

(a) Effect of substrate traverse speed and mechtrode rotational speed on corrosion resistance

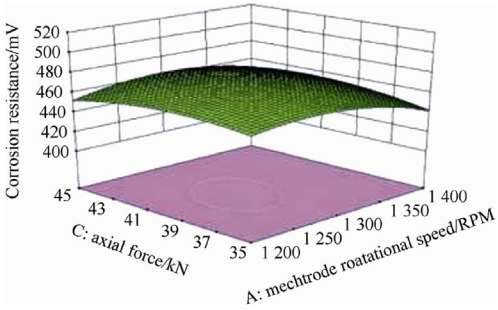

(b) Effect of axial force and mechtrode rotational speed on corrosion resistance

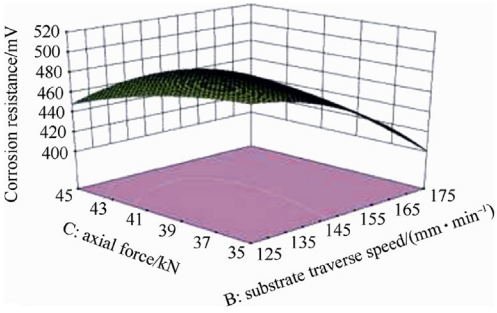

(c) Effect of axial force and substrate traverse speed on corrosion resistance

Fig. 13. Response surfaces for pitting corrosion resistance.

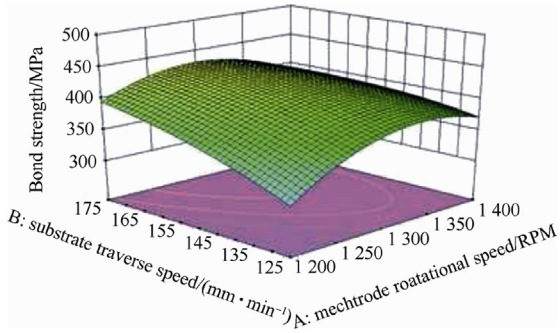

(a) Effect of substrate traverse speed and mechtrode rotational speed on bond strength

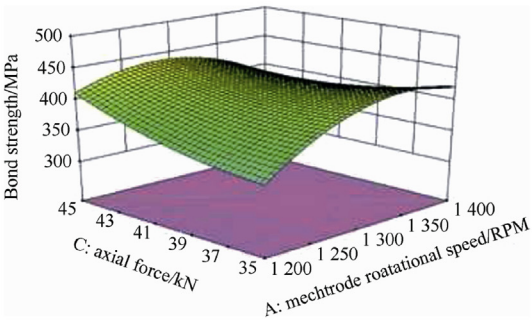

(b) Effect of axial force and mechtrode rotational speed on bond strength

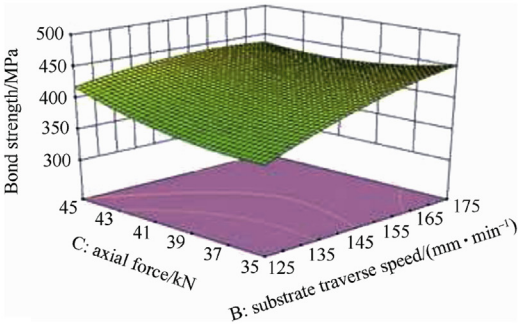

(c) Effect of axial force and substrate traverse speed on bond strength

Fig. 14. Response surfaces for bond strength.

and substrate) and substrate geometry result in a complex process response [20]. The adequacy of the models developed is tested by using the analysis of variance (ANOVA) which is presented in Table 4. The R^2 values for both responses (0.88 for bond strength and 0.71 for corrosion resistance) are more than 0.70 which implies that at least 70% of the variability in the data for each response is explained by the models. The response values are used to compute the model coefficients by using the least square method. After the determination of the significant coefficients, the final model is developed using these coefficients.

Regression analysis of the data in the form of regression equation is presented in Table 5.

Table 4
ANOVA table for the responses.

Response	Source	Sum of squares	df	Mean square	*F* value	*P* value
Bond strength	Regression	74612.93	9	8290.32	8.62	0.0011
	Residual error	9613.26	10	961.32		
	Total	84226.2	19			
Corrosion resistance	Regression	33274.45	9	3697.16	3.07	0.047
	Residual error	12027.75	10	1202.77		
	Total	45302.2	19			

Contour plots play a very important role in the study of the response surface. If a contour patterning of circular shaped contours occurs, it tends to suggest the independence of factor effects, while other shapes may indicate factor interactions [11]. In this study the contour lines for all two factors suggest that the interaction effect is significant. Fig. 13 illustrates the relationship between the pitting corrosion resistane of coating and process parameters. Response surface of corrosion resistance for mechtrode rotational speed (A) and substrate traverse speed(B) shows a gradual increase in output value with substrate traverse speed(B) for all values of mechtrode rotational speed (A). The general trend observed from Fig. 14 is that the increase in rotational speed would decrease the bond strength for a given substrate traverse speed; however for a given rotational speed the increase in traverse speed would tend to increase the bond strength. For the given rotational speed, the increase in axial force on mechtrode would result in the increase in bond strength.

The optimization capability in design expert software was used to optimize the input process parameters for obtaining the maximum pitting corrosion resistance and bond strength of friction surfaced coating. The maximum pitting corrosion resistance was predicted by using the surface model with

Table 5
Regression equations for response functions.

Response	Regression equation
Bond strength	$417.09 + 12.94A + 24.94B + 7.81C - 17.62AB - 26.37AC - 16.37BC - 40.08\ A^2 - 10.83\ B^2 - 13.42C^2$
Pitting corrosion resistance	$493.5 + 0.49A + 2.62B + -2.25C - 23AB - 24.5AC - 17.75BC - 27.87A^2 - 12.87\ B^2 - 2C^2$

A – mechtrode rotational speed, B – substrate traverse speed, C – axial load on mechtrode.

mechtrode rotational speed of 1215 rpm, substrate traverse speed of 135 mm/s and axial load of 35 kN, and the maximum bond strength was predicted by using the response surface model with mechtrode rotational speed of 1325 rpm, substrate traverse speed of 165 mm/s and axial load of 45 kN.

Confirmation experiments were conducted using the optimum setting parameters of bond strength and pitting corrosion resistance. The optimum setting parameters were found to be within the confidence interval of the predicted optimal bond strength and pitting corrosion resistance.

4. Conclusions

The present work shows that austenitic stainless steel AISI 304 can be readily friction surfaced on high strength low alloy steel substrate with excellent coating/substrate bonding. Coatings in the as-deposited condition shows strain-induced martensite in austenitic matrix. Pitting resistance of surfaced coating was found to be much lower than that of mechtrode material and superior to that of substrate. The model developed in the present work based on response surface methodology has been found to be an effective method for the identification and development of significant relationships among process variables and coating properties. From the results of optimization, it was observed that the low and intermediate levels of substrate traverse speed and mechtrode rotational speed and the higher values of axial force produced the optimum bond strength.

Acknowledgments

Financial assistance from Defence Research Development Organization is gratefully acknowledged. The authors would like to thank Dr. Amol A Gokhale, Director and Outstanding scientist, Defence Metallurgical Research Laboratory, Hyderabad, India for his continued encouragement and permission to publish this work.

References

[1] Chandrasekaran M, Batchelor AW, Jana S. Study of interfacial phenomena during friction surfacing of mild steel with tool steel and inconel. J Material Sci 1998;88:2709−17.

[2] Voutchkov I, Jaworski B, Vitanov VI, Bedford GM. An integrated approach to friction surfacing process optimization process. Surf Coat Technol 2001;141:26−33.

[3] Yamashita Yoshihiro, Fujita Kazuhiro. Newly developed repairs on welded area of LWR stainless steel by friction surfacing. J Nucl Sci Technol 2001;38:896−900.

[4] Bedford GM. Friction surfacing for wears applications. Metals Mater 1990;6(11):702−5.

[5] Liu Xuemei, Yao Junshan, Wang Xinhong, Qu ZengdaZou and Shiyao. Finite difference modeling on the temperature field of consumable-rod in friction surfacing. J Mater Process Technol 2009;209:1392−9.

[6] Vitanov VI, Voutchkov I, Bedford GM. Decision support system to optimise the frictec (friction surfacing) process. J Mater Process Technol 2000;107:236−42.

[7] Vitanov VI, Voutchkov II. Process parameters selection for friction surfacing applications using intelligent decision support. J Mater Process Technol 2005;159:27−32.

[8] Madhusudhan Reddy G, Srinivasa Rao K, Mohandas T. Friction surfacing: novel technique for metal matrix composite coating on aluminium−silicon alloy. Surf Eng 2009;2:25−30.

[9] Liu XM, Zou ZD, Zhang YH, Qu SY, Wang XH. Transferring mechanism of the coating rod in friction surfacing. Surf Coat Technol 2008;202:1889−94.

[10] Khalid Rafi H, Janaki Ram GD, Phanikumar G, Prasad Rao K. Microstructural evolution during friction surfacing of tool steel H13. Mater Des 2011;32:82−7.

[11] Montgomery DC. Design and analysis of experiments. 5th ed. New York: John Wiley and Sons; 2001.

[12] Box GEP, Hunter WH, Hunter JS. Statistics for experiments− an introduction to design, data analysis, and model building. 10th ed. New York: John Wiley Publications; 1978.

[13] Mudali UK, Shankar P, Ningshen S, Dayal RK, Khatak HS, Raj B. On the pitting corrosion resistance of nitrogen alloyed cold worked austenitic stainless steels. Corr Sci 2002;44:2183−90.

[14] Raja KS, Rao KP. Pitting behavior of type 17-4 PH stainless steel weldments. Corrosion 1995;51:586−92.

[15] Pickering HW, Frankenthal RP. On the mechanism of localized corrosion of iron and stainless steel: I. Electrochemical studies. J Electrochem Soc 1972;119:1297−304.

[16] Chastell DJ, Doig P, Flewitt PEJ, Norman PJ. Environmental cracking of type 316 austenitic stainless steel weldments in high temperature CO_2 gas. Metall Trans A 1988;19A:1445−51.

[17] Walker RA, Gooch TG. Pitting resistance of weld metal for 22Cr−5Ni ferritic austenitic stainless steel. Br Corros J 1991;26:51−9.

[18] Castrol R, Cadenet JJ. Welding metallurgy of stainless steels. London: Cambridge University Press; 1963.

[19] Enright TJ, Sharp WF, Bergmann OR. Explosive bonding dissimilar metals. Metal Prog ASM July, 1970:107−14.

[20] Pantelis D, Tissandier A, Manolatos P, Ponthiaux P. Formation of wear resistant Al−SiC surface composite by laser melt−particle injection process. Mater Sci Technol 1995;11:299−303.